

SLAC-PUB-7320

October 1996

(A/E/I)

The polarized electron beam for the SLAC Linear Collider

M. Woods

Stanford Linear Accelerator Center
Stanford University, Stanford, CA 94309

Abstract. The SLAC Linear Collider has been colliding a polarized electron beam with an unpolarized positron beam at the Z^0 resonance for the SLD experiment since 1992. An electron beam polarization of close to 80% has been achieved for the experiment at luminosities up to $8 \cdot 10^{29} \text{cm}^{-2} \text{s}^{-1}$. This is the world's first and only linear collider, and is a successful prototype for the next generation of high energy electron linear colliders. This paper discusses polarized beam operation for the SLC, and includes aspects of the polarized source, spin transport and polarimetry.

*Presented at the 12th International Symposium on High Energy Spin Physics
Amsterdam, The Netherlands
September 10-14, 1996*

This work was supported in part by Department of Energy contract DE-AC03-76SF00515

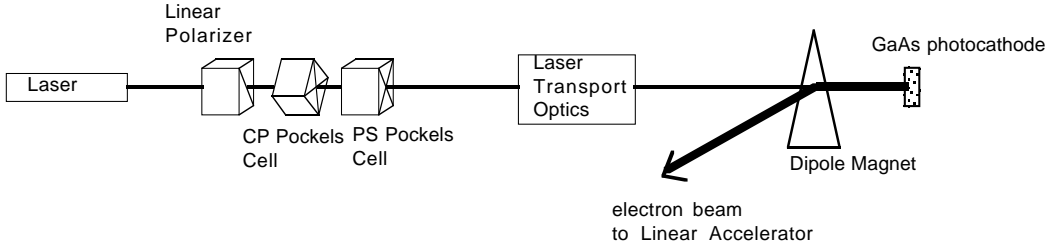


Figure 1: SLAC Polarized Electron Source

A highly polarized electron beam is a key feature for the current physics program at SLAC [1]. Fixed target experiments in End Station A (ESA) study the collision of polarized electrons with polarized nuclear targets to elucidate the spin structure of the nucleon and to provide an important test of QCD. Using the SLAC Linear Collider (SLC), collisions of polarized electrons with unpolarized positrons allow precise measurements of parity violation in the Z -fermion couplings and provide a very precise measurement of the weak mixing angle.

Polarized electrons are produced [2] by photoemission from a GaAs photocathode. For SLC operation, two Nd:YAG-pumped Ti:sapphire lasers produce two 2ns pulses separated by about 60ns. One of these pulses is used to make electrons for collisions, and the other one is used to make electrons for positron production.

The laser is polarized with a linear polarizer and two Pockels cells as shown in Figure 1. The axes of the linear polarizer and the PS Pockels cell are along the x, y axes, while the axes of the CP Pockels cell are along u, v (u, v axes are rotated by 45° with respect to x, y). This configuration can generate arbitrary elliptical polarization, and can compensate for phase shifts in the laser transport optics. The laser circular polarization, \mathcal{P}_γ , at the GaAs photocathode is well approximated by $\mathcal{P}_\gamma = \sin\left(\frac{V_{CP}-V_{CP}^T}{V_{\lambda/4}} \cdot \frac{\pi}{2}\right)\cos\left(\frac{V_{PS}-V_{PS}^T}{V_{\lambda/4}} \cdot \frac{\pi}{2}\right)$, where V_{CP} and V_{PS} are the Pockels cell voltages; $V_{\lambda/4}$ is the Pockels cell quarterwave voltage; V_{CP}^T and V_{PS}^T are phase shifts induced by the laser transport optics. To generate circular polarized light, one nominally operates the CP Pockels cell at its quarterwave voltage and the PS cell at 0 Volts. Small corrections to these voltages are needed to compensate for phase shifts in the transport optics to the photocathode. A positive HV pulse on the CP Pockels cell produces one helicity, while a negative HV pulse produces the opposite helicity. The sign of this HV pulse is set by a pseudo-random number generator, which updates at 120 Hz (the electron beam pulse rate).

The photoexcitation of electrons in *strained* GaAs from the valence band to the conduction band is illustrated in Figure 2. The strain is induced by growing a thin $0.1 \mu\text{m}$ layer of GaAs on GaAsP, and this splits the degeneracy in the $j=3/2$ valence band by about 50 meV. Photons with positive helicity and with energies greater than the band gap energy of 1.43 eV, but less than 1.48 eV excite the transition shown from the $m_j = -3/2$ valence level to the $m_j = -1/2$ conduction level. The extracted electrons from the GaAs cathode have the same helicity as the incident

photons since they have opposite direction to the incident photons (see Figure 1). In principle, one should achieve an electron beam polarization, \mathcal{P}_e , of 100%. But in practice, we only achieve $\mathcal{P}_e \sim 80\%$. The achieved value has been observed to depend on the photocathode quantum efficiency (QE) and on the thickness of the strained layer. How to achieve polarizations closer to 100% is an active research area [3].

Two problems encountered with the GaAs photoelectron source are *Charge Limit* [4] and *Charge Asymmetry* [5]. Charge Limit is a phenomenon whereby the instantaneous photocathode QE decreases appreciably due to high incident light fluxes, and thereby limits the maximum electron charge that can be extracted. Experimentally we find that the maximum extracted charge is proportional to the QE at low incident light fluxes and is independent

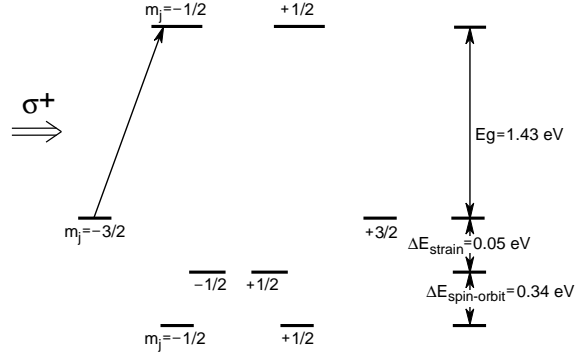


Figure 2: GaAs Energy Levels

of the maximum laser power available. In practice, this has not severely impacted the performance of the polarized electron source at SLAC, but it is an issue that needs to be addressed for photocathode electron sources. The Charge Asymmetry problem results from small linear polarized components in the laser beam and a dependence of the electron yield on the orientation of the linear polarization. For laser light which is 100% linear polarized, 10% variations in the electron yield have been observed depending on the orientation of the linear light polarization. This effect results from anisotropies in the strain [5]. Even light with $\mathcal{P}_\gamma = 99.5\%$ has 10% linear polarization, and appreciable charge asymmetries between the *right* and *left* beam polarization states at the 1% level can result. In practice, this is an easy problem to fix by monitoring the electron beam charge asymmetry and controlling the Pockels cell voltages to null the asymmetry. For the SLAC source, we control the PS Pockels cell voltage to null the charge asymmetry in a feedback loop. It is easy to maintain the asymmetry below 10^{-4} and the level of the average asymmetry is only limited by the sophistication of the feedback algorithm and the statistical fluctuations in the electron charge.

Two electron bunches are produced from the photocathode gun, which operates at 120 kV. This high voltage is needed to increase the *space charge limit* current capability of the gun above the 6 amps of peak current needed for SLC operation. The gun is a complex device where high voltage arcing and poor vacuum can easily destroy the photocathode QE. Additionally, the photocathode requires careful preparation to achieve a negative electron affinity surface to produce an adequate QE. A very large effort was mounted at SLAC to achieve a robust photocathode electron gun; details of the gun design and operation can be found in Reference [2].

A schematic of the SLC is shown in Figure 3. Two electron bunches from the photocathode gun are injected into the SLAC Linear Accelerator (Linac) where they are bunched and accelerated to 1.19 GeV. They are then kicked by a pulsed magnet into the Linac-to-Ring (LTR) transfer line to be transported to the electron damping ring (DR). The DR stores the beam for 8ms to reduce the beam emittance. The Ring-to-Linac (RTL) transfer line transports the two bunches from the DR and a pulsed magnet kicks them back into the Linac.

These two bunches are preceded down the Linac by a positron bunch which has been extracted from the positron DR. Three bunches are accelerated down the Linac. The trailing electron bunch is accelerated only to 30 GeV, and is sent to the positron production target. Positrons in the energy range 2-20 MeV are collected, accelerated to 200 MeV, and transported to near the start of the Linac for transport to the positron DR, where they are damped for 16 ms. At the end of the Linac, the electron and positron energies are each 46.6 GeV. A magnet deflects the electron (positron) bunch into the north (south) collider arc for transport to the Interaction Point (IP). In the arcs, the beams lose about 1 GeV in energy from synchrotron radiation so that the resulting center-of-mass collision energy is 91.2 GeV, which is chosen to match the Z^0 mass. The beam energies are measured with energy spectrometers with an accuracy of 20 MeV.

The electron spin orientation is longitudinal at the source and remains longitudinal until the LTR transfer line to the electron DR. In the LTR, the electron spin precesses by 450° to become transverse at the entrance to the LTR spin rotator solenoid. This solenoid rotates the electron spin to be vertical in the DR to preserve the polarization. The spin orientation is vertical upon extraction from the DR; it remains vertical during injection into the Linac and during acceleration to 46.6 GeV down the Linac.

The SLC arc transports the electron beam from the Linac to the IP and is comprised of 23 achromats, each of which consists of 20 combined function magnets. At 46.6 GeV, the spin precession in each achromat is 1085° , while the betatron phase advance is 1080° . The SLC arc is therefore operating near a spin tune resonance. A result of this is that vertical betatron oscillations in the horizontal bends of the arc's achromats can

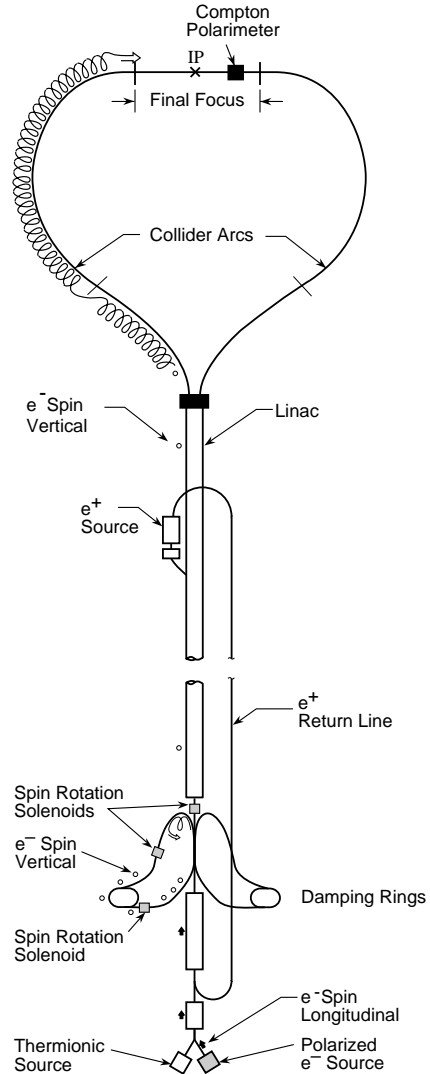


Figure 3: The Polarized SLC

cause the beam polarization to rotate away from vertical; this rotation is a cumulative effect in successive achromats. (The rotation of the vertical spin component in a given achromat is simply due to the fact that rotations in x and y do not commute, while the cumulative effect is due to the spin resonance.) The resulting spin component in the plane of the arc then precesses significantly.

The arc's spin tune resonance, together with misalignments and complicated rolls in the arc, result in an inability to predict the spin transport through the arc. However, we have two good experimental techniques for orienting the spin longitudinally at the IP. First, using the RTL and Linac spin rotator solenoids one can orient the electron spin to be along the x , y , or z axis at the end of the Linac. The z -component of the arc's spin transport matrix can be measured with the Compton polarimeter [6], which measures the longitudinal electron polarization,

$$P_z^C = R_{zx} \cdot P_x^L + R_{zy} \cdot P_y^L + R_{zz} \cdot P_z^L$$

The experimental procedure is referred to as a 3-state measurement, and is accomplished by measuring P_z^C for each of x , y , or z spin orientations at the end of the Linac. The arc spin rotation matrix elements R_{zx} , R_{zy} , R_{zz} are then determined. This is sufficient to determine the full rotation matrix, which is described by three Euler angles. The matrix R can be inverted to determine the required spin orientation at the end of the Linac for the desired longitudinal orientation at the IP. This is achieved with appropriate settings of the RTL and LINAC spin rotators.

A second method to orient the spin longitudinally at the IP takes advantage of the arc's spin tune resonance. A pair of vertical betatron oscillations ('spin bumps'), each spanning 7 achromats in the last third of the arc, are introduced to rotate the spin. The amplitudes of these spin bumps are empirically adjusted to achieve longitudinal polarization at the IP. Thus, the two spin bumps can effectively replace the two spin rotators. For the 1992 SLD run, the spin rotator magnets were used to orient the electron beam polarization at the IP. But since 1993, spin bumps have been used instead because the SLC is now colliding flat beams to achieve higher luminosity and the spin rotators introduce unacceptable x - y coupling [7].

The Compton polarimeter measures the average electron beam polarization, \mathcal{P}_e , which can differ from by a small amount from the luminosity-weighted beam polarization, $\mathcal{P}_e(1 + \xi)$. The dominant effect is a chromatic one: the electron beam has a finite energy spread $n(E)$; the spin orientation of the electron beam has an energy dependence $\theta_S(E)$; and chromatic aberrations in the final focus result in a luminosity dependence on beam energy, $L(E)$. The beam energy spread is monitored by automated wire scans at a high dispersion point. These are done frequently since the energy distribution of the beam can easily change. The dependence of the spin orientation and luminosity on the beam energy are more stable. During the 1994/5 SLD run, 4 measurements of $\theta_S(E)$ were made. Estimates of $L(E)$ are made by 3 techniques: simulations of the final focus optics, measurements of beam spotsizes versus energy, and measurements of the Z boson production rate for off-energy pulses. These three estimators give consistent results, with the measured

data having somewhat less energy dependence than the simulations. We use our determinations of $n(E)$, $\theta_S(E)$ and $L(E)$ to estimate the chromatic contribution to ξ . For the 1994/95 SLD run, we find this contribution to be $+0.0020 \pm 0.0014$. An additional effect of similar magnitude arises from the small precession of the electron spin in the final focusing quadrupoles, which for the 1994/95 run contributed -0.0011 ± 0.0001 to ξ . We have also measured depolarization due to beam-beam effects and find this to be 0.000 ± 0.001 , consistent with theoretical predictions [8]. Combining these 3 effects, we find $\xi = +0.0009 \pm 0.0017$ for the 1994/95 SLD run.

The average luminosity-weighted electron beam polarization for the 1994/95 SLD run was $(77.2 \pm 0.5)\%$. The SLD experiment is approved to continue running with a polarized electron beam through 1998. Additionally, there will be a fixed target experiment, E155, with polarized beam in the spring of 1997. Future running of SLD and ESA experiments in parallel with B factory operation at SLAC are also being considered.

- [1] M. Woods, *AIP Conference Proceedings* **343**, 230 (1995). (Proceedings of SPIN94)
- [2] R. Alley et al., *Nucl. Inst. Meth.* **A365**, 1 (1995).
- [3] Experimental and theoretical discussions of maximizing the electron polarization for GaAs photocathodes were held at the SPIN96 Pre-Symposium *Workshop on polarized electron sources and low energy polarimeters*; see proceedings.
- [4] M. Woods et al., *J. Appl. Phys.* **73**, 8531 (1993); H. Tang et al., SLAC-PUB-6515 (1994).
- [5] R.A. Mair et al., *Phys. Lett.* **A212**, 231 (1996).
- [6] M. Woods, SLAC-PUB-7319 (1996), contributed to these proceedings.
- [7] T. Limberg, P. Emma, and R. Rossmanith, SLAC-PUB-6210 (1993).
- [8] K. Yokoya, P. Chen, SLAC-PUB-4692 (1988).